M.TECH DISSERTATION REPORT

ON

NUMERICAL SIMULATION OF NiTi/Al FIBER REINFORCED MATRIX COMPOSITE

BY

VINODHKUMAR V

(2015PDE5458)

UNDER THE SUPERVISION OF

DR. AMIT SINGH

DEPARTMENT OF MECHANICAL ENGINEERING,

MALAVIYA NATIONAL INSTITUE OF TECHNOLOGY,

JAIPUR-302017 (RAJASTHAN).

2016-2017

A

DISSERTATION REPORT

ON

NUMERICAL SIMULATION OF NiTi/Al FIBER REINFORCED MATRIX COMPOSITE

Submitted in partial fulfillment of the requirements for the award of degree of

MASTER OF TECHNOLOGY
IN
DESIGN ENGINEERING

Submitted By	**Supervised by**
Vinodhkumar V	**Dr. Amit Singh**
(2015PDE5458)	(Assistant Professor)

DEPARTMENT OF MECHANICAL ENGINEERING,

MALAVIYA NATIONAL INSTITUTE OF TECHNOLOGY,

JAIPUR-302017 (RAJASTHAN).

2016-2017

DEPARTMENT OF MECHANICAL ENGINEERING,

MALAVIYA NATIONAL INSTITUTE OF TECHNOLOGY,

JAIPUR-302017 (RAJASTHAN).

CERTIFICATE

This is to certify that the dissertation work entitled "Numerical Simulation of NiTi/Al Fiber Reinforced Matrix Composite" by Mr. Vinodhkumar V is a bonafide work completed under my supervision and guidance, and hence approved for submission to the Department of Mechanical Engineering, Malaviya National Institute of Technology in partial fulfillment of the requirements for the award of the degree of Master of Technology with specialization in Design Engineering. The matter embodied in this Seminar Report has not been submitted for the award of any other degree, or diploma.

Place: Jaipur **Dr. Amit Singh**

Date: 04 Jul 2017 **(Assistant professor)**

DEPARTMENT OF MECHANICAL ENGINEERING,
MALAVIYA NATIONAL INSTITUTE OF TECHNOLOGY,
JAIPUR-302017 (RAJASTHAN).

Candidate's Declaration

I hereby certify that the work which is being presented in the dissertation entitled "Numerical Simulation of NiTi/Al Fiber Reinforced Matrix Composite", in partial fulfilment of the requirements for the award of the Degree of Master of Technology in Design Engineering, submitted in the Department of Mechanical Engineering, MNIT, Jaipur is an authentic record of my own work carried out for a period of one year under the supervision of Dr. Amit Singh, Assistant professor of Mechanical Engineering Department, MNIT, Jaipur.

I have not submitted the matter embodied in this dissertation for the award of any other degree.

Place: Jaipur **Vinodhkumar V**

Date: 04 Jul 2017 **M. Tech (DE)**

ID: 2015PDE5458

Acknowledgement

I express sincere thanks to my supervisor Dr. Amit Singh, Assistant Professor, Department of Mechanical Engineering, M.N.I.T.,Jaipur., for providing me his invaluable guidance, support, supervision and useful suggestions. I am sincerely thankful to Dr. Dinesh Kumar Singh, Dr. T.C. Gupta and Dr. Himanshu Choudhary who helped me beyond their duty at time of need.

Home is where one starts from; I express my deepest gratitude to my parents and my younger brother for sharing their love. The motivation they rendered in times of need is limitless which lets one achieve above and beyond.

Place: Jaipur
Date: 04 Jul 2017

Vinodhkumar V
M. Tech (DE)
ID: 2015PDE5458

Abstract

This thesis studies the improvement in residual stress of the shape memory alloy (SMA). It mainly focuses on the simulation of three composite models NiTi/Al, Ni/Al and Ti/Al. ANSYS workbench is used in the simulation process. The metal matrix composite fiber reinforced with SMA materials since it is possible to prolong the fatigue life of the component by reducing the residual stress of the composite material. It is a proven fact that the compressive stress equals to be good stress for the matrix composite material which enhances the material properties. The mismatch of thermal expansion and the compressive residual stress between the fibre (NiTi) and matrix (Al) is studied.

Shape Memory Alloys (SMA) on thermal loading makes use of the compressive residual stress generated while loading to get back to its original shape and size. This effect is studied in ANSYS Workbench version 16.2 and Finite element analysis is conducted on all three metal matrix composite.

Table of Contents

List of Figures

List of Tables

Nomenclature

SMA	Shape Memory Alloy
TTR	Transformation Temperature Range
SME	Shape Memory Effect
FEM	Finite Element Method
FEA	Finite Element Analysis
a	Length of SMA
b	Width of SMA matrix
h	Thickness of matrix
E	Young's modulus
Al	Aluminum
Ni	Nickel
Ti	Titanium

Chapter-1

Introduction

1.1 Shape Memory Alloys (SMAs)

SMAs are a group of alloys that can restructure to their original form (shape or size) on subjecting to a memorization process between two transformation phases. This phenomenon is called as Shape Memory Effect (SME).

In 1932, the solid phase Change in SMA was discovered by Arne Olander, a Swedish physicist who determined that the gold-cadmium (Au–Cd) alloys could be plastically deformed on cooling, and gets back to the original configuration when heated. However many observations were presented over the period of years it was Dr. William J. Buehler a researcher at the Naval Ordnance Laboratory, White Oak, Maryland saw the potential to commercialize SMA applications after discovering NiTi alloy. NiTinol (Nickel, titanium) alloys are cheaper to produce, easier and safer to handle, and have better mechanical properties compared to other existing SMA.

SMA shows the restoring force when it is heated beyond a specific phase transformation temperature range (TTR) after deformation at a temperature lower than the inherent mechanical "memory" or TTR. This phenomenon is caused by reversible metamorphosis from austenite to the "parent" mechanically formed Martensitic (also known as stress-induced martensite). [1].

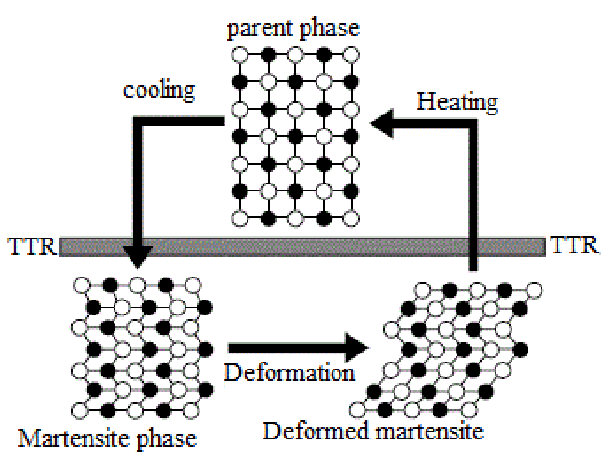

Fig. 1. Schematic of Crystal Structure[2]

1.1.1 Applications of SMA's

SMA's finds its applications in a variety of fields. Some of them are given below.

i. Automotive applications
   a. Sensors and actuators
   b. Car engine compartment
   c. Vehicle door (grab) Handle
ii. Aerospace Applications
   a. actuators
   b. structural connectors
   c. vibration dampers
iii. Robotic applications
   a. micro-actuators or artificial muscles
   b. Actuators in robotic finger
   c. Biomimetics
iv. Biomedical applications
   a. endodontics
   b. medical tweezers
   c. implants
   d. eyeglass frames

Table 1. Composition of some SMAs (Janke et al. 2005)

Alloy	Composition
Ni-Ti	49-51 Ni
Ni-Ti-Cu	8-20 Cu
Ni-Al	36-38 Al
Fe-Ni-Nb	31 Ni, 7 Nb
Fe-Ni-Co-Ti	33 Ni, 10 Co, 4 Ti
Cu-Al-Ni	28-29 Al, 3-4.5 Ni
Cu-Zn	38.5-41.5 Zn

1.1.2 Advantages and Fabrication techniques of SMA’s

SMA’s are largely used in different fields because of the following advantages [2]:

- Larger tolerances on mating parts.
- Low-temperature installation.
- Accurate and predictable stresses.
- Wide operating temperature range and lower installed cost.

When it comes to the fabrication process of SMAs many techniques such as electron-beam melting, vacuum arc melting or vacuum induction melting are employed [3].

Table 2: Alloys exhibiting the shape memory effect [4]

S.N.	Alloys
1	Au-Cd
2	Cu-Zn
3	In-Ti
4	Ni-Ti
5	Cu-Zn-Al
6	Ti-Nb

7	Au-Cu-Zn
8	Cu-Zn-Sn
9	Cu-Zn-Si
10	Ag-Cd
11	Cu-Sn
12	Cu-Zn-Ga
13	Ni-Al
14	Fe-Pt
15	U-Nb
16	Ti-Pd-Ni
17	Fe-Mn-Si
18	Cu-Al-Ni

1.2 Nickel Titanium Naval Ordinance Laboratory (NiTiNoL)

NiTinol, which stands for Nickel Titanium Naval Ordnance Laboratory, was discovered by Dr. William J. Buehler a researcher at the Naval Ordnance Laboratory in White Oak, Maryland during the year 1961. This SMA known for its unique behavior under mechanical and thermal loads have been used in various applications.

NiTinol has the ability to show thermally recoverable deformation on the order of 6% or more strain. In the SM stage beneath certain temperature, NiTinol displays stiffness similar to soft copper wire to get desired shape and size. Fig 2, depicts upon increase in temperature post deformation NiTinol, the material gets back to its original shape by correcting its undergone deformation.

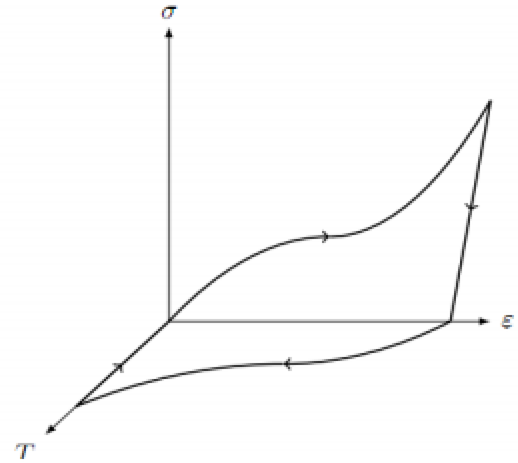

Fig. 2. **NiTinol deformation and temperature induced recovery [3]**

NiTinol phase depends on configuration of crystal structure of Nickel and Titanium. The structurally stiff austenite phase occurs at high temperature, whereas the martensite phase occurring at lower temperature is not stiff like austenite. Fig 3, depicts martensite in a twinned configuration. Upon loading it becomes detwinned and it retains the strain induced. On increase of temperature sufficiently phase change to austenite is induced, returning the material to the original shape [5]

`

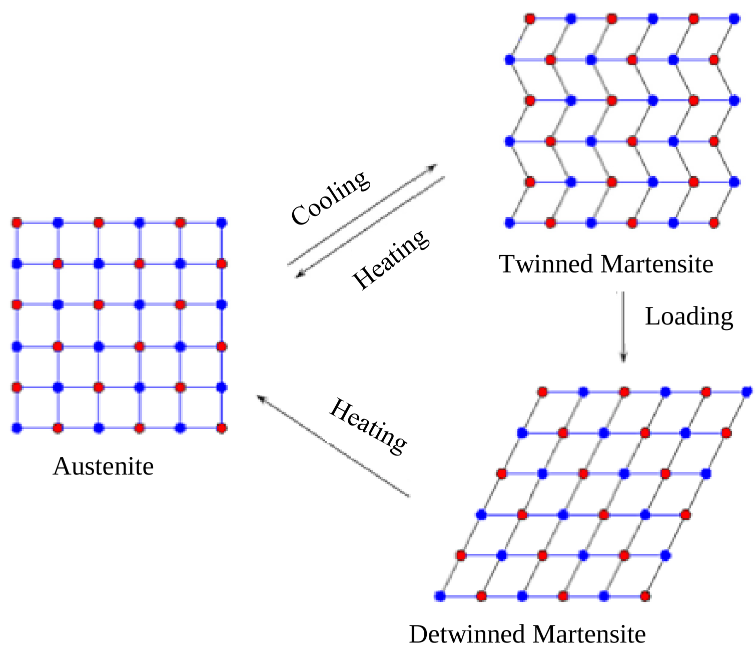

Fig. 3. **Phases of NiTinol and their process relation**

NiTi is an increasingly applicable material in commercial programs. Owing to difficulties in welding and joining limits its production of complex shapes. The primary weldability issues associated with NiTi are the strength reduction, alteration of segment transformation and modifications in both deformation temperature and ultra-elastic and form reminiscence effect. Similarly, NiTi is supposed to be bonded with different substances, a greater hassle that depends on other substrates, hence affecting the weld and its impact at the overall performance of the fittings. As a latest development, laser welding technique is employed in fusion of NiTi [6].

Chapter-2

Literature review and objectives

2.1 There exist strong demands for materials that have the high mechanical properties. Akira Shimamoto a, Hiroshi Ohkawara b, Fumio Nogata developed a design concept that improves the material strength. SMA property is used to control the material strength. TiNi shape memory fiber-reinforced epoxy matrix composite is used as test specimen, to analyse the effectiveness of the new concept. The test was conducted by the photoelastic method. The photo-elastic fringe patterns and the behavior of K-value at the crack tip validate the effectiveness of the proposed design concept. Then, an analytical model based on Eshelby's model is developed in order to compute the average matrix compressive stress [7].

Watanabe ae al, proposed a fabrication method using for producing a shape memory alloy (SMA) to be used in civil engineering applications. At room temperature, the Fe–Mn–Si–Cr SMA fibers are subjected to pre-tensile strain to form plaster matrix. The composites of Fe–Mn–Si–Cr are heated to 250^{o}C to cause a compressive residual stress in the matrix. The bonding strength at SMA fibre and plaster matrix interface is found out by conducting a fibre pull-out test. FEA is perfomed to have further insights on the results made available experimentally. It is identified that the bonding strength of the composites increases with increasing level of pre-tensile strain. By using cheap Fe–Mn–Si–Cr SMA fibers for the reinforcement of the SMA composite, materials for practical engineering applications can be acquired at low cost [8].

Jamian, Saifulnizan et al proposed another technique for the Equal channel Angle Press (ECAP) to prepare materials that are hard to handle. By combining materials that are hard to work with and those that are easy to work with, the latter will help working the material that is easy to work with. The ECAP procedure is recreated by FEM. In this study Ti (hard to work) metal is taken and embedded into Al (easy to work) material. The strain distribution of this phenomenon is studied using FEM [9].

Choon, Tan Wee, Salleh, Abdul Saad, Jamian, Saifulnizan, and Mohd. Imran Ghazali studies the phase transformation temperature of the SMA. The essential parameter for

SMA is Phase transformation temperature. The popular method that exists to determine this Phase transformation temperature is Differential Scanning Calorimeter (DSC). Another novel method employed for the same is universal testing machine. These experiments are tested in this review material [10].

Petrini, Lorenza et al studied Ni–Ti alloys that are more widely used in bioengineering applications. The two main thermo-mechanical behaviors i.e. the shape memory effect and the pseudoelastic effect were studied along with other properties of SMA's such as resistance to corrosion, fatigue resistance, biocompatibility, etc. They enable Ni–Ti alloys to experience mechanically incited deformation and to recover to original shape by thermal loading or mechanical unloading. In this paper the scientists created a numerical model is created to get the most critical SMA perceptible thermo-mechanical properties and is implemented into a commercial component to simulate the performance of in biomedical applications. The SMA's behavior in recovering to the original shape after thermal loading is studied [11].

Song Xiaoyun et al found that NiTiAl base combination is a potential high-temperature basic material drawing attention in various engineering applications. Alloying is a successful way to enhance their mechanical properties. The microstructure and mechanical properties of this alloy has been investigated by various methods such as X-ray diffraction (XRD), Scanning electron microscopy (SEM), and pressure test in this paper. The effect of Mo is evident by rise of yield strength and decrease in plasticity. This paper studies the microstructure and mechanical property of NiTiAl and concludes that presence of Mo in this alloy precipitation strengthening effect [12].

L.J. Zheng et al, studied the newly designed NiTiAlNb alloy to find the precipitation type and its hardness relationship. Cyclic tensile loading and unloading is carried out to observe the deformation behaviour. The new phase designed with approximate composition increases the hardness of the alloy and followed by cyclic loading that generates a linear strain which is recoverable whose value increased more than 3%. Thus increasing the load bearing capability of the alloy [13].

V. I. Itin et al, reviewed the mechanical properties and shape memory effect of TiNi alloys for prosthesis and healing. The porous nature provides excellent bone fixation of the living tissues. The biocompatibility property lets these substances perform for a long time in the body without being removed. Powder sintering and ignition synthesis, the two methods of manufacturing are described here. The porous TiNi alloys manufactured using these methods exhibit super elastic property and have enhanced shape memory effect. Under certain conditions, these parameters approach the parameters of solid alloys. The yield strength, SME and stored recoverable strain are controlled by porosity [14].

Liu, K.T. et al studied Ni50.5Ti49.5 and Ni45.6Ti49.3Al5.1 thin films were fabricated by direct current (DC) magnetron sputtering and post-annealed at 773, 798, 823, 873 and 923 K. The crystallization kinetics was investigated by differential scanning calorimetry (DSC). Hardness and grain size of nickel-titanium-aluminium films annealed at different temperature were evaluated by nano-indentation test and X-ray diffactometer (XRD). The peak hardness of Ni45.6Ti49.3Al5.1 film was 12.9 GPa at 823 K, which was significantly improved as compared to Ni50.5Ti49.5 film with only 8.8 GPa. Hardness of both deposited and heat treated Ni45.6Ti49.3Al5 film increased with the amount of aluminium due to the effect of solid solution in the nickel-titanium system. The appropriate annealing temperature for specific Ni45.6Ti49.3Al5 film was selected at 823 K on the basis of the hardness consideration [15].

Liu, K.T. et al studied the effect of aluminium on the corrosion behavior of NiTiAl thin films. An electrochemical research for study of corrosion behavior using Potentiodynamic and Tafel technology, 0.9% NaCl Solution on TiNi and Ni-Ti-Al shape memory thin films. Applied Atomic force microscopy (AFM) and electron probe Micro Analyzer (EPMA) was observing the form of each of the surface film and the element distribution after dipping and before immersing in 0.9% NaCl solution. The Dissolved NI concentration from Ni-Ti-Al thin films in electrolytes measured by inductively coupled plasma atomic emission spectrometry (Aes), compared with the TI thin film. It is observed that after immersion for seven days concentration of Ni from Ni-Ti-Al is significantly much lesser. Thin films will be potentially beneficial to biological applications. This quality enhancement is attributed to introduction of aluminum in the compostion [16].

Gashti, S. O. et al selected a nanostructured Ni–Ti–Al system through mechanothermal process. This study throws light upon the structural and morphological evaluation of mechanically alloyed powders. The result exhibited that, the aluminum dissolved into NiTi structure after mechanical alloying helps in obtaining the low crystalline NiTi(1 1 0) phase. The milled powders transformed into nanocrystalline NiTiAl and Ni3(Ti,Al) phases after annealing at 1150°C for 15 min. According to XRD patterns, SEM micrographs and TEM results, the mechanothermal process can be used for preparation of nanostructured Ni–Ti–Al system which, otherwise, cannot be made through conventional methods with appropriate structural and morphological features [17].

Loong, Tang Tsz Process-induced residual stress in shape memory alloy (SMA) fiber reinforced aluminum (Al) matrix composite was simulated by ANSYS APDL. The manufacturing process of the composite named as NiTi/Al is start with loading and unloading process of nickel titanium (NiTi) wire as SMA to generate a residual plastic strain. Then, this plastic deformed NiTi wire would be embedded into Al to become a composite. Lastly, the composite is heated frrm 289 K to 363 K and then cooled back to 300 K. Residual stress is generated in composite because of shape memory effect of NiTi and mismatch of thermal coefficient between NiTi wire and Al matrix of composite. ANSYS APDL has been used to simulate the distribution of residual stress and strain in this process. A sensitivity test has been done to determine the optimum number of nodes and elements used. Hence, the number of nodes and elements used are 15680 and 13680, respectively. Furthermore, the distribution of residual stress and strain of nickel fiber reinforced aluminium matrix composite (Ni/Al) and titanium fiber reinforced aluminium matrix composite (Ti/Al) under same simulation process also has been simulated by ANSYS APDL as comparison to NiTi/Al. The simulation results show that compressive residual stress is generated on Al matrix of Ni/Al, Ti/Al and NiTi/Al during heating and cooling process. Besides that, they also have similar trend of residual stress distribution but difference in term of value. For Ni/Al and Ti/Al, they are 0.4% difference on their maximum compressive residual stress at 363K. At same circumstance, NiTi/Al has higher residual stress value which is about 425% higher than Ni/Al and Ti/Al composite. This implies that shape memory effect of NiTi fiber reinforced in composite able to generated higher compressive residual stress in Al matrix, hence able to enhance tensile property of the composite [18].

In summary, applications of SMAs seen increased acceptance in a wide variety of industries around the world. Attempts are in progress by researchers around the world to learn complete features of SMAs, and to develop acceptable material models.

2.2 Objectives

- To study the shape memory alloys (SMA) as it's highly useful in various engineering and biomedical applications.
- The Ni/Al, Ti/Al and Ni-Ti/Al fibre matrix composite fibres are designed.
- The material properties are assigned and is subjected to load ranging from 160N to 260N
- The equivalent elastic strain generated is observed using Finite Element Technique in ANSYS work bench.
- The enhancement of SME in NiTi/Al fibre matrix composite as compared to Ni/Al and Ti/Al is studied.

Chapter-3

Approach and problem formulation

3.1 Finite Element Analysis:

3.1.1 Need for FEA:

The traditional design process and stress analysis techniques can be applied to the satisfaction only in the range of a conventional part shape and a specific load condition by using a sound theory. The design process requires continuous improvement to get a final product that will be of satisfying quality to the customer. This is how the product will be standardized. Certain geometric parameters are changed to achieve the optimum design and the desired function from the product. Therefore, conventional design techniques are not so useful for frequent changes in design calculations.

For eg, Expansion joints are customized products, which needs to be treated individually for various applications. The design procedure is carried out carefully and requires minor modifications. Traditional design process gives rise to many ambiguities due to diverse application areas of expansion joints. Thus, designers normally use higher safety factors in order to minimize risk. This leads to over design components by specifying either unnecessarily bulky cross sections or high quality materials. Inevitably the cost of the product increases which is not a warranted condition in the industry. Finite Element Analysis (FEA) provides a better solution for design and stress analysis in the virtual environment.

3.1.2 Introduction to FEA:

Finite Element Analysis (FEA) is a computer-based numerical technique for calculating the strength and behavior of engineering structural components. It can be used to calculate deflection, stress, vibration, buckling behavior and many other phenomena. It can be used to analyze either small or large scale deflection under loading or applied displacement. It can analyze elastic deformation, as well as plastic deformation. Finite element analysis makes it possible to evaluate in detail the complex structures, in a computer, during the planning of the structure. The demonstration of adequate strength of the structure and the possibility of improving the design during planning can justify the need of this analysis work.

The first issue to understand in FEA is that it is fundamentally an approximation. The underlying mathematical model may be an approximation of physical system. The finite element itself approximates what happens in its interior with the help of interpolating formulas.

In the finite element analysis, first step is modeling. Using any special CAD software, model can be generated using the construction and editing features of the software. In finite element method the structure is broken down into many small simple blocks called elements. The material properties and the governing relationships are considered over these elements. The behavior of an individual element can be described with a relatively simple set of equations. Just as the set of elements would be joined together to build the whole structure, the equations describing the behavior of the individual.

Elements are also joined into an extremely large set of equations that describe the behavior of whole structure. The computer can solve large set of simultaneous equations. From the solutions, the computer extracts the behavior of the individual elements. From this, it can get the stress and deflection of all parts of a structure. The stresses will be compared to permissible values of stress for the materials to be used, to see if the structures are strong enough.

Interpretation of the results requires knowing what is an acceptable approximation, development of a complete list of what should be evaluated; appreciation of the need of margin of safety, and comprehension of what remains unknown after an analysis.

There are many software available for finite element analysis, which can be utilized for the engineering applications. They are ANSYS & Pro/Engineer.

3.1.3 Overview of FEA Procedure:

The basic steps in the finite element method are

1 Discretize the region of interest.

Divide the problem domain into a number of finite subdomains each of simple geometry Each subdomain called element has a number of nodal points, the locations m space of which are given m coordinates relative to a set of global axes The shape of each element is defined in terms of these co-ordinates by interpolation or shape functions.

2 Assume a variation of the unknown.

An interpolation function is proposed for the variation of the unknown (eg displacement, temperature) inside each element in terms of values at the nodes These interpolation functions in many cases are the same as the shape functions used to describe the element shape

3 Find element response matrices.

For each element, coefficient matrices which describe the response characteristics of the element are determined In solid mechanics applications, for example, a matrix of stiffness coefficients is computed In order to determine the stiffness matrix the material behaviour has to be defined

4 Assemble the element matrices.

To find the stiffness matrix of the whole problem domain, the stiffness matnces of the individual elements are combined This forms a matrix equation expressing the behaviour of the entire solution Region

5 Solve the system of equations

In most problems the number of equations is large, thus special solution techniques are employed After solution the values of the dependent variables at all the nodes of the domain are known

6 Determine other variables

Using the nodal values and interpolation functions, other parameters such as strain, stress etc inside each element may be determined

3.2 Problem definition:

3.2.1 Geometric model for Simulation

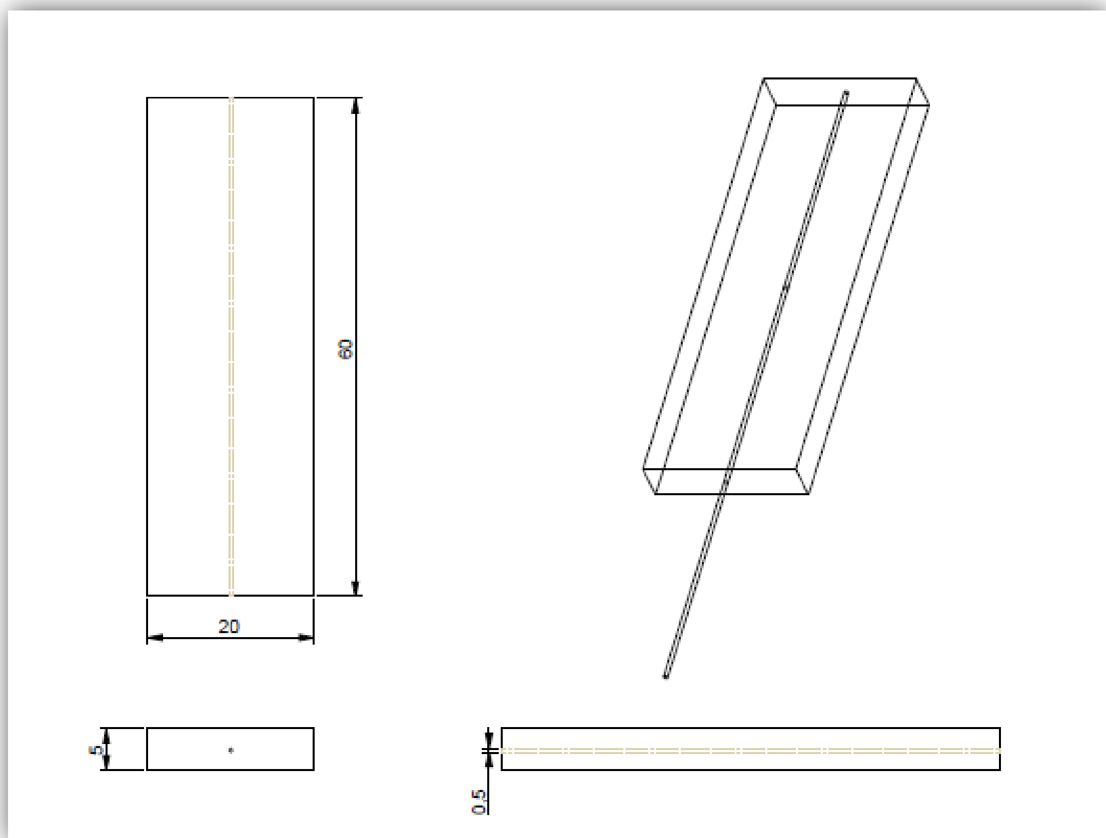

Fig 4. **Dimensions of the Ni-Ti/Al fibre matrix composite.**

The NiTi fibre/wire of size 0.5 mm is embedded into Al matrix of 60 mm length, 20 mm width and 5 mm depth.

3.2.2 Type of Mesh:

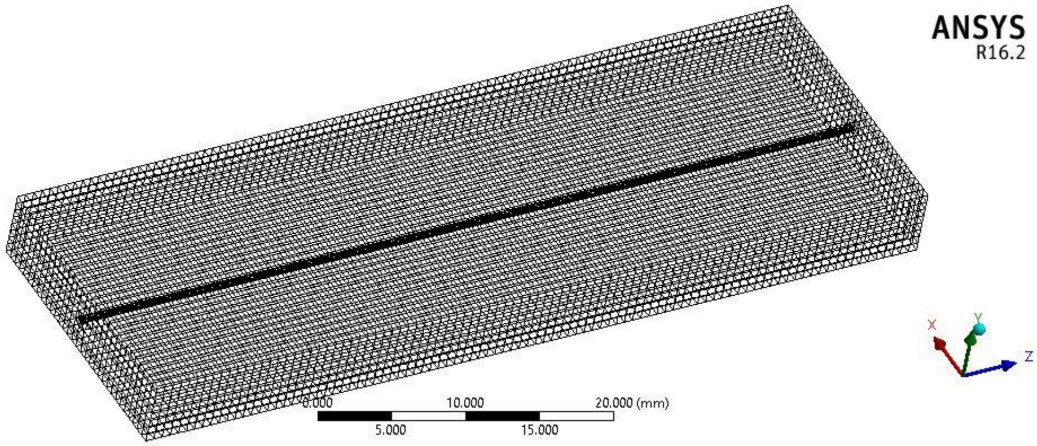

Fig 5. **The sample post meshing**

The mesh designates the cells or elements on which the problem is solved. It is a discrete representation of the geometry of the problem. For solving this problem hexahedron cell type is chosen for meshing which is a type of multi-block meshing. In this the mesh density is high enough to capture all the relevant flow features. Skewness, smoothness and aspect ratio are the three measures of mesh quality that on improving produce better results.

The types of mesh include structured grid, unstructured mesh and multiblock,

3.3 Grid independent test:

Grid dependence study is performed to eliminate/reduce the influence of the number of grids/grid size on the computational results. It is a good practice to follow this study for every individual geometry. The grid dependence for geometry will be applicable only for that particular geometry.

(a) Grid independent test and mesh convergence study are the same.

(b) The solution obtained is never correct unless the grid/mesh is converged to an acceptable level of tolerance.

(c) When the no of meshes/grid points are increased the error in numerical solution will decrease and the agreement between the obtained solution and the exact experimental results will be better.

(d) The study here is conducted on the metal matrix composite to find the number of nodes and elements where the error rate will be zero. The optimum number thus found is 570 elements and 3350 nodes.

3.3.1 **Steps Followed:**

(a) Run the simulation on intial mesh obtained and study the convergence of residual error.

(b) Now improve the mesh and repeat the simulation to ensure that the error drops to 0 and the imbalances are below 1%.

(c) Compare the solution obtained at step 2 with the solution obtained at step 1. If the value is same then mesh employed at step 1 is virtuous enough to capture the result.

(d) If the solution changes because of mesh resolution then it is considered that the solution is not independent of the mesh. As solution varies with refinement of mesh, a solution independent of the mesh is yet to be achieved. Now improve the mesh and repeat the process until we have a solution independent of the grid resolution.

Table 3. Grid independent test

MESH (GRID) INDEPENDENT TEST OF THREE COMPOSITES (rod)			
Element	**Node**	**Relevance Factor**	**Error (%)**
98	714	10	2
176	1189	20	1.99
254	1664	0	1.42
332	2139	50	1.16
410	2614	70	0.4
456	2945	80	0.36
488	3089	90	0.15
570	3350	100	0
744	3657	100	0
814	3892	100	0
844	4512	100	0
890	4887	100	0
920	5112	100	0
950	5378	100	0
997	5681	100	0
1123	5723	100	0
1367	5987	100	0

The material properties of Aluminium, nickel, titanium are extracted from the ansys workbench library. The details of the properties used to conduct the analysis are listed as below,

	A	B	C	D
1	Contents of Engineering Data		ource	Description
2	Material			
3	Aluminum Alloy			General aluminum alloy. Fatigue properties come from MIL-HDBK-5H, page 3-277.
4	Nickel			Fatigue Data at zero mean stress comes from 1998 ASME BPV Code, Section 8, Div 2, Table 5-110.1
5	Nickel Titanium			Fatigue Data at zero mean stress comes from 1998 ASME BPV Code, Section 8, Div 2, Table 5-110.1
6	Titanium Alloy			
*	Click here to add a new material			

Properties of Outline Row 3: Aluminum Alloy

	A	B	C	D	E
1	Property	Value	Unit		
2	Density	2770	kg m^-3		
3	Isotropic Secant Coefficient of Thermal Expansion				
6	Isotropic Elasticity				
16	Alternating Stress R-Ratio	Tabular			
20	Tensile Yield Strength	2.8E+08	Pa		
21	Compressive Yield Strength	2.8E+08	Pa		
22	Tensile Ultimate Strength	3.1E+08	Pa		
23	Compressive Ultimate Strength	0	Pa		

Fig 6. **Properties of Aluminium [19]**

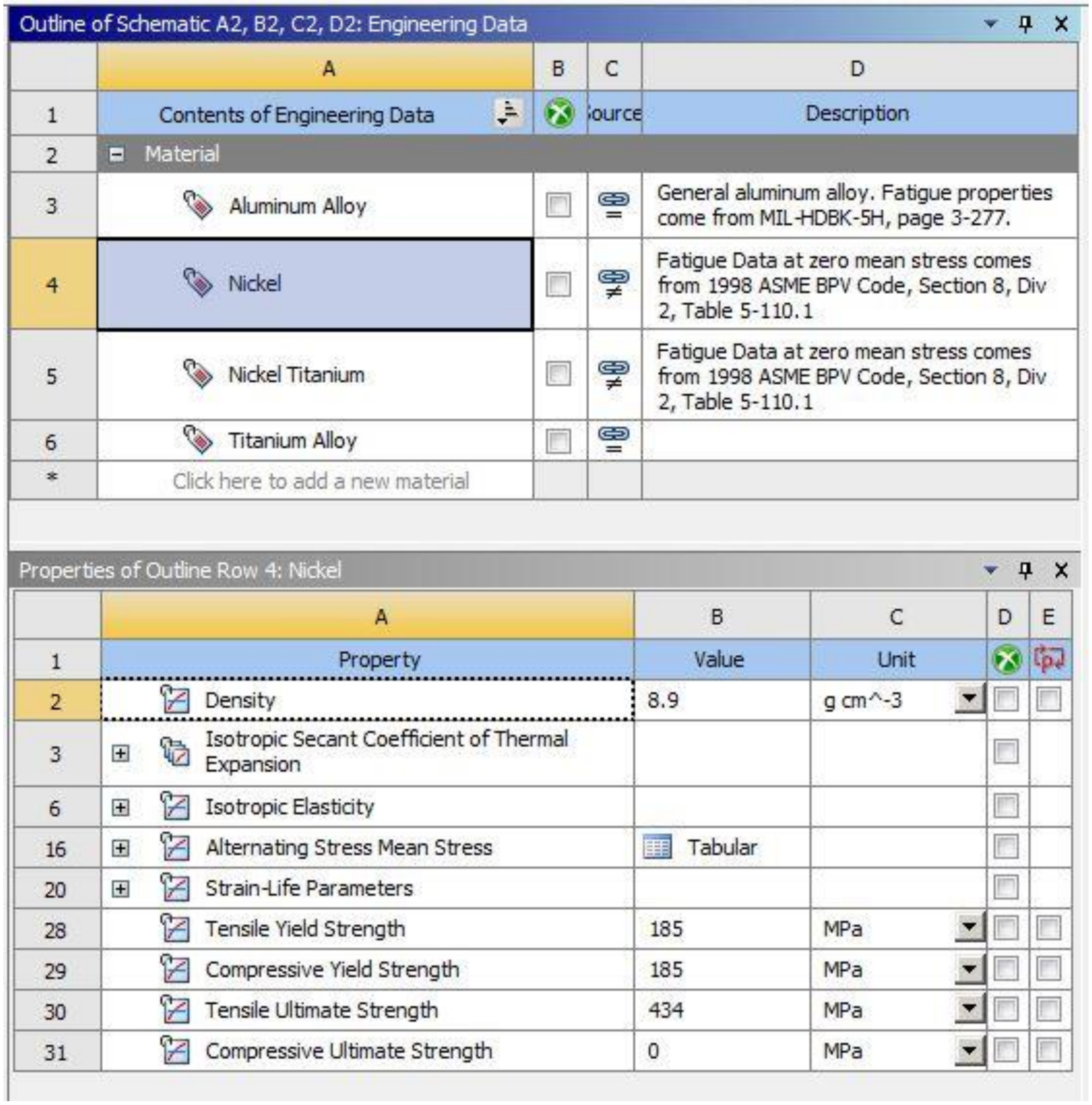

Outline of Schematic A2, B2, C2, D2: Engineering Data

	A	B	C	D
1	Contents of Engineering Data		ource	Description
2	Material			
3	Aluminum Alloy			General aluminum alloy. Fatigue properties come from MIL-HDBK-5H, page 3-277.
4	Nickel			Fatigue Data at zero mean stress comes from 1998 ASME BPV Code, Section 8, Div 2, Table 5-110.1
5	Nickel Titanium			Fatigue Data at zero mean stress comes from 1998 ASME BPV Code, Section 8, Div 2, Table 5-110.1
6	Titanium Alloy			
*	Click here to add a new material			

Properties of Outline Row 4: Nickel

	A	B	C	D	E
1	Property	Value	Unit		
2	Density	8.9	g cm^-3		
3	Isotropic Secant Coefficient of Thermal Expansion				
6	Isotropic Elasticity				
16	Alternating Stress Mean Stress	Tabular			
20	Strain-Life Parameters				
28	Tensile Yield Strength	185	MPa		
29	Compressive Yield Strength	185	MPa		
30	Tensile Ultimate Strength	434	MPa		
31	Compressive Ultimate Strength	0	MPa		

Fig 7. **Properties of Nickel [20]**

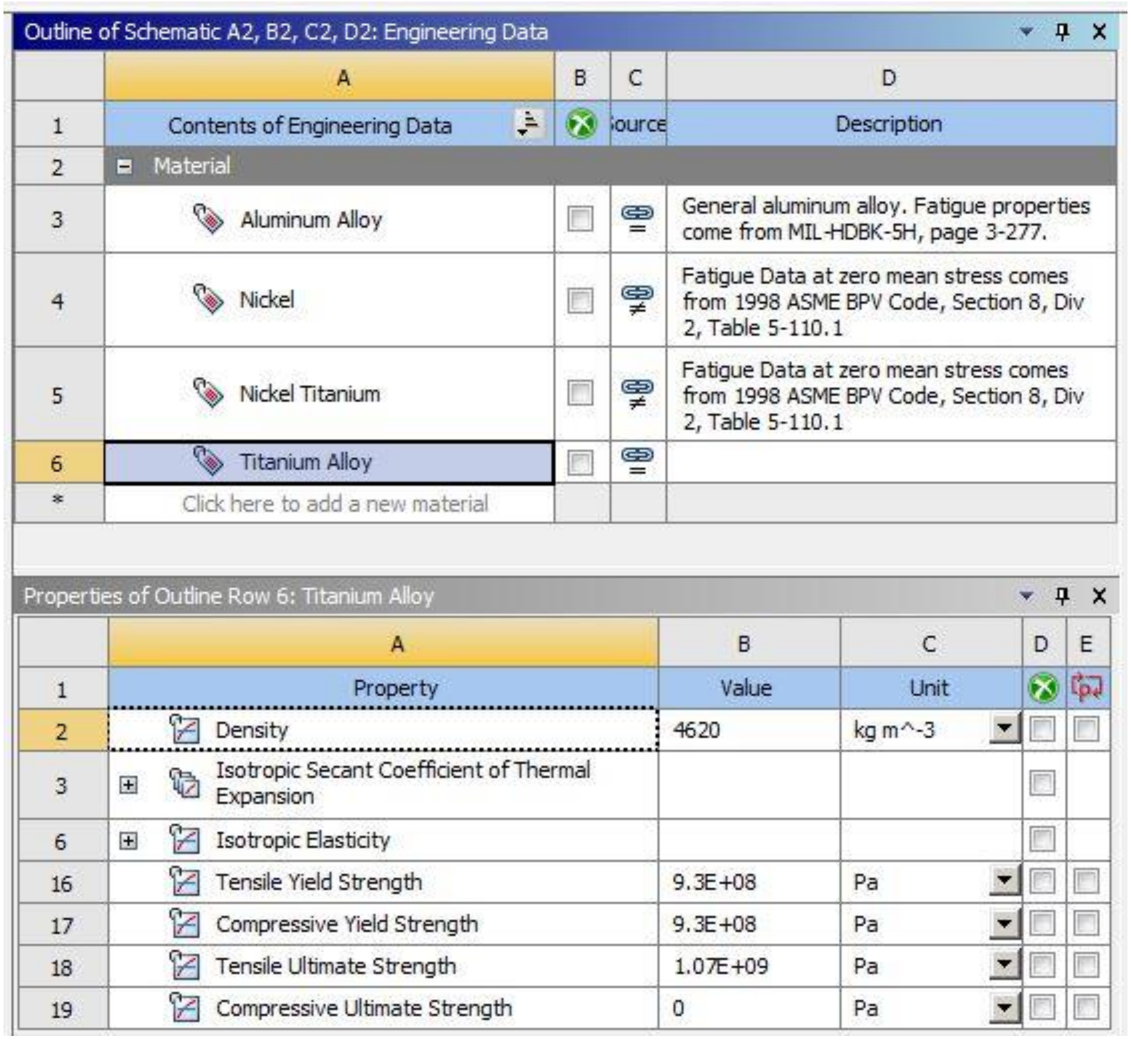

Outline of Schematic A2, B2, C2, D2: Engineering Data

	A	B	C	D
1	Contents of Engineering Data		Source	Description
2	Material			
3	Aluminum Alloy			General aluminum alloy. Fatigue properties come from MIL-HDBK-5H, page 3-277.
4	Nickel			Fatigue Data at zero mean stress comes from 1998 ASME BPV Code, Section 8, Div 2, Table 5-110.1
5	Nickel Titanium			Fatigue Data at zero mean stress comes from 1998 ASME BPV Code, Section 8, Div 2, Table 5-110.1
6	Titanium Alloy			
*	Click here to add a new material			

Properties of Outline Row 6: Titanium Alloy

	A	B	C	D	E
1	Property	Value	Unit		
2	Density	4620	kg m^-3		
3	Isotropic Secant Coefficient of Thermal Expansion				
6	Isotropic Elasticity				
16	Tensile Yield Strength	9.3E+08	Pa		
17	Compressive Yield Strength	9.3E+08	Pa		
18	Tensile Ultimate Strength	1.07E+09	Pa		
19	Compressive Ultimate Strength	0	Pa		

Fig 8. **Properties of Titanium**

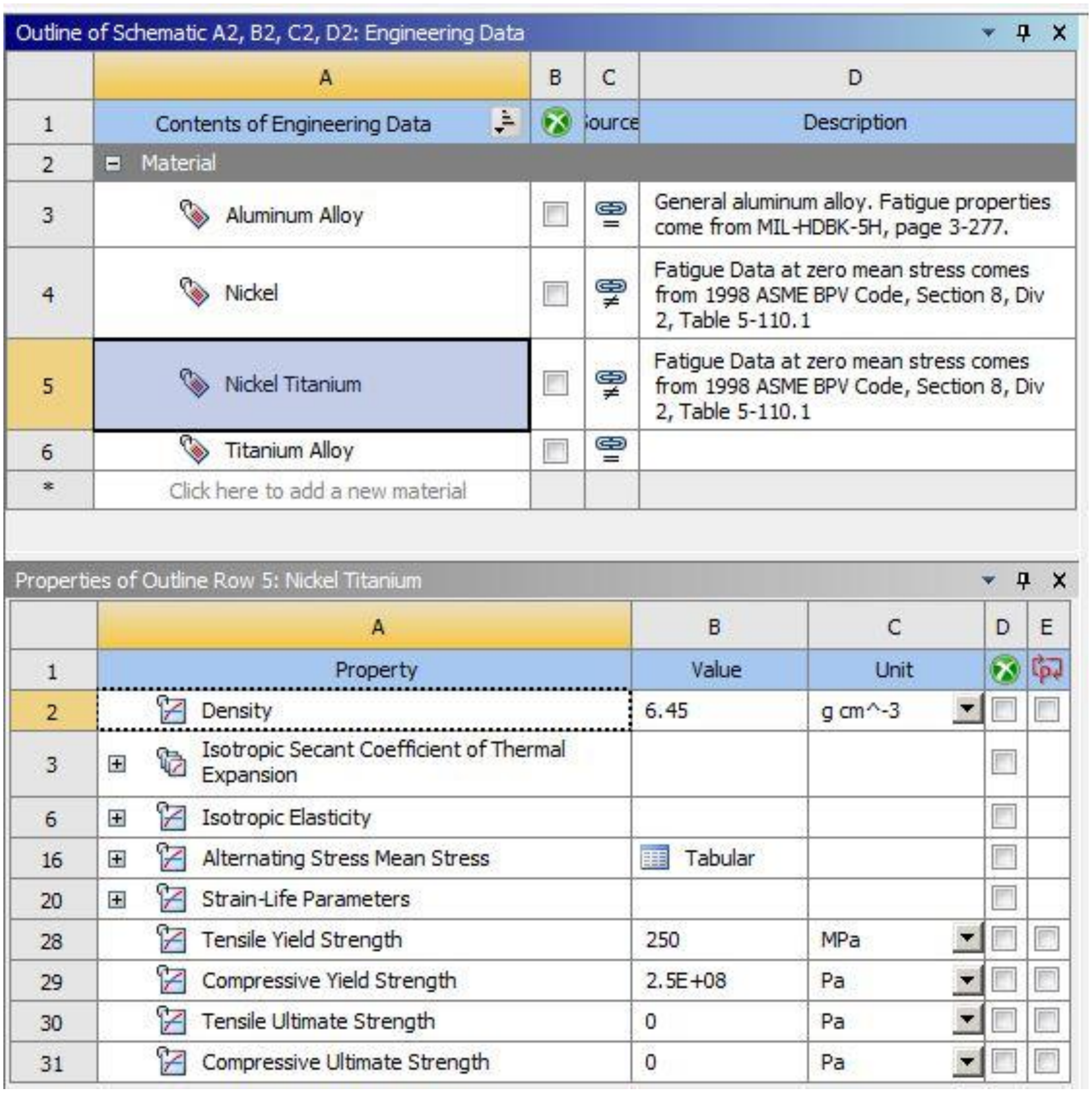

Outline of Schematic A2, B2, C2, D2: Engineering Data

	A	B	C	D
1	Contents of Engineering Data		Source	Description
2	Material			
3	Aluminum Alloy			General aluminum alloy. Fatigue properties come from MIL-HDBK-5H, page 3-277.
4	Nickel			Fatigue Data at zero mean stress comes from 1998 ASME BPV Code, Section 8, Div 2, Table 5-110.1
5	Nickel Titanium			Fatigue Data at zero mean stress comes from 1998 ASME BPV Code, Section 8, Div 2, Table 5-110.1
6	Titanium Alloy			
*	Click here to add a new material			

Properties of Outline Row 5: Nickel Titanium

	A	B	C	D	E
1	Property	Value	Unit		
2	Density	6.45	g cm^-3		
3	Isotropic Secant Coefficient of Thermal Expansion				
6	Isotropic Elasticity				
16	Alternating Stress Mean Stress	Tabular			
20	Strain-Life Parameters				
28	Tensile Yield Strength	250	MPa		
29	Compressive Yield Strength	2.5E+08	Pa		
30	Tensile Ultimate Strength	0	Pa		
31	Compressive Ultimate Strength	0	Pa		

Fig 9. **Properties of Nickel-Titanium [21]**

3.4 Meshing details of NiTi/Al:

The meshing details such as unit measurement, geometry, parts and mesh contacts are described as follows

Table 4. Unit Measurement

Unit System	Metric (mm, kg, N, s, mV, mA) Degrees rad/s Celsius
Angle	Degrees
Rotational Velocity	rad/s
Temperature	Celsius

3.4.1 Geometry

Table 5. Geometry

Object Name	*Geometry*
State	Fully Defined
Definition	
Type	DesignModeler
Length Unit	Meters
Bounding Box	
Length X	20. mm
Length Y	5. mm
Length Z	60. mm
Properties	
Volume	6000. mm^3
Scale Factor Value	1.
Statistics	
Bodies	2
Active Bodies	2
Nodes	117569
Elements	25840
Mesh Metric	None
Basic Geometry Options	
Parameters	Yes
Parameter Key	DS
Attributes	No
Named Selections	No
Material Properties	No
Advanced Geometry Options	
Use Associativity	Yes

Coordinate Systems	No
Reader Mode Saves Updated File	No
Use Instances	Yes
Smart CAD Update	No
Compare Parts On Update	No
Attach File Via Temp File	Yes
Analysis Type	3-D
Decompose Disjoint Geometry	Yes
Enclosure and Symmetry Processing	Yes

3.4.2 Parts Description

Table 6. Parts

Object Name	***ROD***	***PANEL***
State	Meshed	
Graphics Properties		
Visible	Yes	
Transparency	1	
Definition		
Suppressed	No	
Coordinate System	Default Coordinate System	
Reference Temperature	By Environment	
Material		
Assignment	Nickel Titanium	Aluminum Alloy
Nonlinear Effects	Yes	
Thermal Strain Effects	Yes	
Bounding Box		
Length X	0.5 mm	20. mm
Length Y	0.5 mm	5. mm
Length Z	60. mm	
Properties		
Volume	11.781 mm³	5988.2 mm³
Mass	7.5987e-005 kg	1.6587e-002 kg
Centroid X	-1.5255e-018 mm	-1.8419e-016 mm
Centroid Y	-7.9717e-002 mm	1.5604e-004 mm
Centroid Z	1.4702e-015 mm	1.8652e-016 mm
Moment of Inertia Ip1	2.2682e-002 kg·mm²	5.0109 kg·mm²
Moment of Inertia Ip2	2.2682e-002 kg·mm²	5.5303 kg·mm²
Moment of Inertia Ip3	2.3506e-006 kg·mm²	0.58862 kg·mm²
Statistics		
Nodes	3350	114219
Elements	570	25270
Mesh Metric	None	

3.4.3 Coordinated systems

Table 7. Mesh

Object Name	***Global Coordinate System***
State	Fully Defined
Definition	
Type	Cartesian
Coordinate System ID	0.
Origin	
Origin X	0. mm
Origin Y	0. mm
Origin Z	0. mm
Directional Vectors	
X Axis Data	[1. 0. 0.]
Y Axis Data	[0. 1. 0.]
Z Axis Data	[0. 0. 1.]

3.4.4 Mesh Details

Table 8. Mesh controls

Object Name	***Contact Region***
State	Fully Defined
Scope	
Scoping Method	Geometry Selection
Contact	2 Faces
Target	2 Faces
Contact Bodies	ROD
Target Bodies	PANNEL
Definition	
Type	Bonded
Scope Mode	Automatic
Behavior	Program Controlled
Trim Contact	Program Controlled
Trim Tolerance	0.15861 mm
Suppressed	No
Advanced	
Formulation	Program Controlled
Detection Method	Program Controlled
Penetration Tolerance	Program Controlled
Elastic Slip Tolerance	Program Controlled

Normal Stiffness	Program Controlled
Update Stiffness	Program Controlled
Pinball Region	Program Controlled
Geometric Modification	
Contact Geometry Correction	None
Target Geometry Correction	None

3.5 Meshing Details of Ni-Al and Ti-Al

Table 9. Unit Measurement

Unit System	**Metric (mm, kg, N, s, mV, mA) Degrees rad/s Celsius**
Angle	Degrees
Rotational Velocity	rad/s
Temperature	Celsius

3.5.1 Geometry

Table 10. Geometry of Ni-Al and Ti-Al

Geometry	Ti-Al	Ni-Al
Object Name	Geometry	Geometry
State	Fully Defined	Fully Defined
Definition		
Type	DesignModeler	DesignModeler
Length Unit	Meters	Meters
Element Control	Program Controlled	Program Controlled
Display Style	Body Color	Body Color
Bounding Box		
Length X	20. mm	20. mm
Length Y	5. mm	5. mm
Length Z	60. mm	60. mm
Properties		
Volume	6000. mm^3	6000. mm^3
Mass	1.6642e-002 kg	1.6642e-002 kg
Scale Factor Value	1	1
Statistics		
Bodies	2	2
Active Bodies	2	2

Nodes	117569	117508
Elements	25840	26834
Mesh Metric	None	None
Basic Geometry Options		
Parameters	Yes	Yes
Parameter Key	DS	DS
Attributes	No	No
Named Selections	No	No
Material Properties	No	No
Advanced Geometry Options		
Use Associativity	Yes	Yes
Coordinate Systems	No	No
Reader Mode Saves Updated File	No	No
Use Instances	Yes	Yes
Smart CAD Update	No	No
Compare Parts On Update	No	No
Attach File Via Temp File	Yes	Yes
Analysis Type	3-D	3-D
Decompose Disjoint Geometry	Yes	Yes
Enclosure and Symmetry Processing	Yes	Yes

3.5.2 Parts Description

Table 11. Parts

Object	**Ti-Al**		**Ni-Al**	
part	**ROD**	**PANEL**	**ROD**	**PANEL**
State	Meshed		Meshed	
Graphics Properties				
Visible	Yes		Yes	
Transparency	1		1	
Definition				
Suppressed	No		No	
Stiffness Behavior	Flexible		Flexible	
Coordinate System	Default Coordinate System		Default Coordinate System	
Reference Temperature	By Environment		By Environment	
Material				

Assignment	Titanium	Aluminum	Nickel	Aluminum
Nonlinear Effects	Yes		Yes	
Thermal Strain Effects	Yes		Yes	
Bounding Box				
Length X	0.5 mm	20. mm	0.5 mm	20. mm
Length Y	0.5 mm	5. mm	0.5 mm	5. mm
Length Z	60. mm		60 mm	
Properties				
Volume	11.781 mm³	5988.2 mm³	11.781 mm³	5988.2 mm³
Mass	5.4428e-005 kg	1.6587e-002 kg	5.4428e-005 kg	1.6587e-002 kg
Centroid X	-1.5255e-018 mm	-1.8419e-016 mm	-1.5255e-018 mm	-1.8419e-016 mm
Centroid Y	-7.9717e-002 mm	1.5604e-004 mm	-7.9717e-002 mm	1.5604e-004 mm
Centroid Z	1.4702e-015 mm	1.8652e-016 mm	1.4702e-015 mm	1.8652e-016 mm
Moment of Inertia Ip1	1.6246e-002 kg·mm²	5.0109 kg·mm²	1.6246e-002 kg·mm²	5.0109 kg·mm²
Moment of Inertia Ip2	1.6246e-002 kg·mm²	5.5303 kg·mm²	1.6246e-002 kg·mm²	5.5303 kg·mm²
Moment of Inertia Ip3	1.6837e-006 kg·mm²	0.58862 kg·mm²	1.6837e-006 kg·mm²	0.58862 kg·mm²
Statistics				
Nodes	3350	114219	3289	114219
Elements	570	25270	1564	25270
Mesh Metric	None			

3.5.3 Coordinate system of Ni-Al & Ti-Al

Table 12. Mesh coordinates

Object Name	Global Coordinate System
State	Fully Defined
Definition	
Type	Cartesian
Coordinate System ID	0.
Origin	
Origin X	0. mm
Origin Y	0. mm
Origin Z	0. mm
Directional Vectors	
X Axis Data	[1. 0. 0.]
Y Axis Data	[0. 1. 0.]
Z Axis Data	[0. 0. 1.]

3.5.4 Mesh Details

Table 13. Mesh controls

Object Name	*Mesh*
State	Solved
Display	
Display Style	Body Color
Defaults	
Physics Preference	Mechanical
Relevance	100
Sizing	
Use Advanced Size Function	Off
Relevance Center	Fine
Element Size	Default
Initial Size Seed	Active Assembly
Smoothing	Medium
Transition	Fast
Span Angle Center	Coarse
Minimum Edge Length	0.78540 mm
Inflation	
Use Automatic Inflation	None
Inflation Option	Smooth Transition
Transition Ratio	0.272
Maximum Layers	5

Growth Rate	1.2
Inflation Algorithm	Pre
View Advanced Options	No
Patch Conforming Options	
Triangle Surface Mesher	Program Controlled
Patch Independent Options	
Topology Checking	No
Advanced	
Number of CPUs for Parallel Part Meshing	Program Controlled
Shape Checking	Standard Mechanical
Element Midside Nodes	Program Controlled
Straight Sided Elements	No
Number of Retries	Default
Extra Retries For Assembly	Yes
Rigid Body Behavior	Dimensionally Reduced
Mesh Morphing	Disabled
Defeaturing	
Pinch Tolerance	Please Define
Generate Pinch on Refresh	No
Automatic Mesh Based Defeaturing	On
Defeaturing Tolerance	Default
Statistics	
Nodes	117569
Elements	25840
Mesh Metric	None

Chapter-4

Finite Element Analysis of the NiTi/Al fibre matrix.

4.1 Analysis

The FEA is carried out on the NiTi/Al fibre matrix after assigning the material properties as stated in the previous chapters. The three composite Ni/Al, Ti-Al and NiTi/Al are designed and its material properties are assigned. The analysis reveals that the SMA Ni-Ti displays enhanced shape retrieval due to its SME.

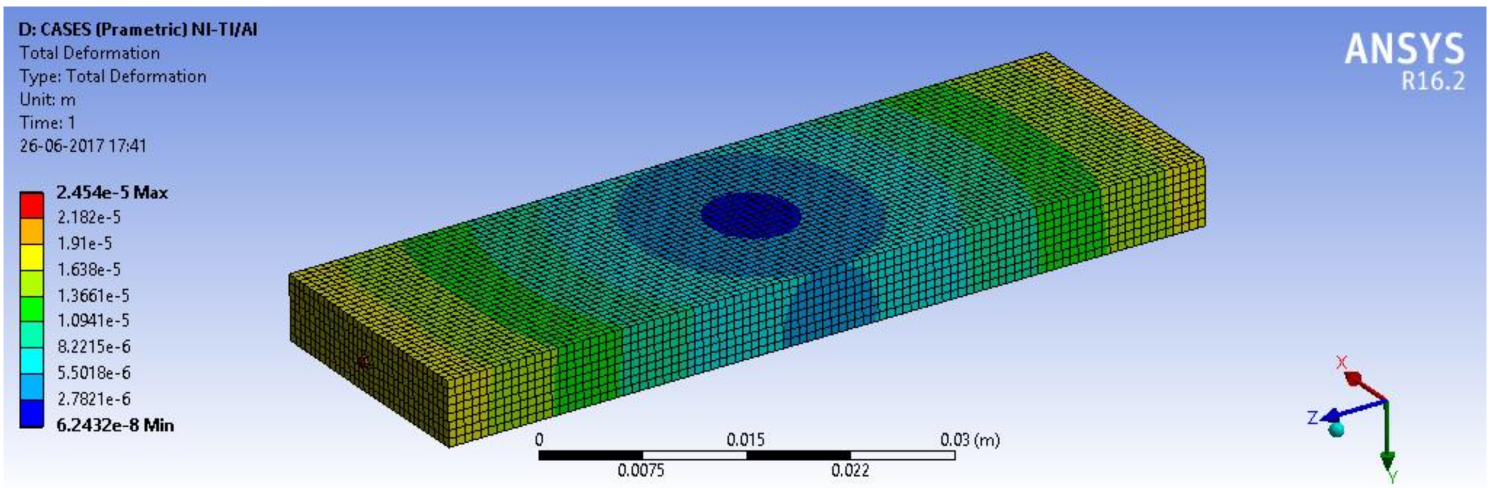

Fig.10 **Total deformation of NiTi/Al**

The shape retrieval on removal of the tensile loading happens at 351K as compared to 363K in the research paper that is taken for this study. The maximum deformation occurs is $2.45*10^{-5}$ m. The thermal loading, eq. elastic strain generated and other parameters taken into consideration over the course of simulation are presented as follows,

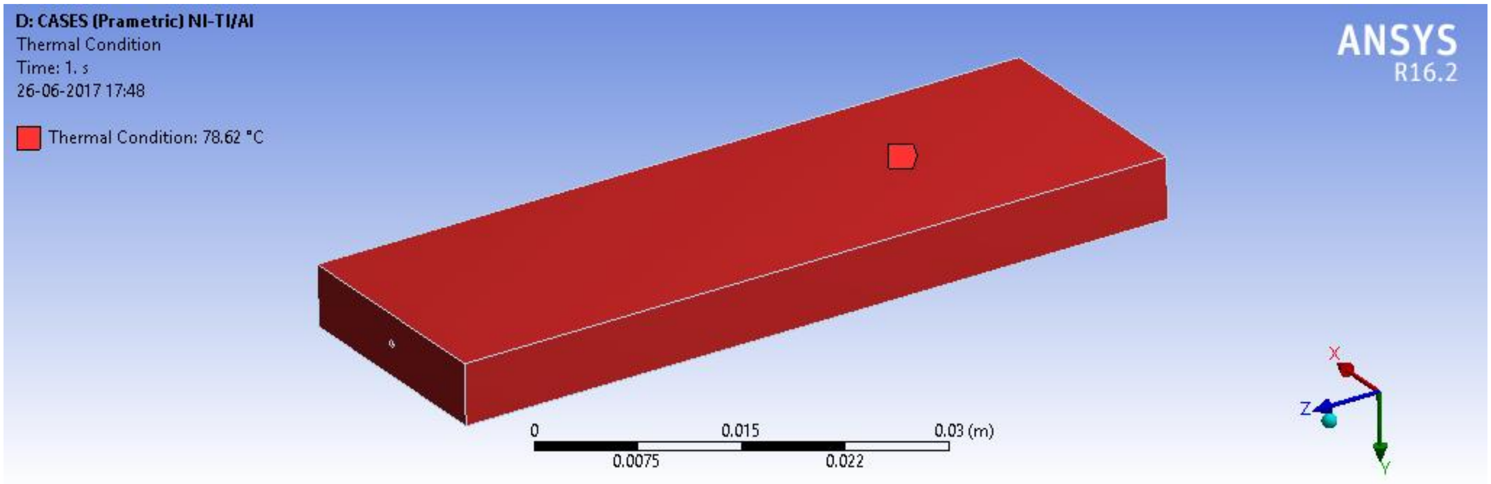

Fig 11. **Thermal Condition**

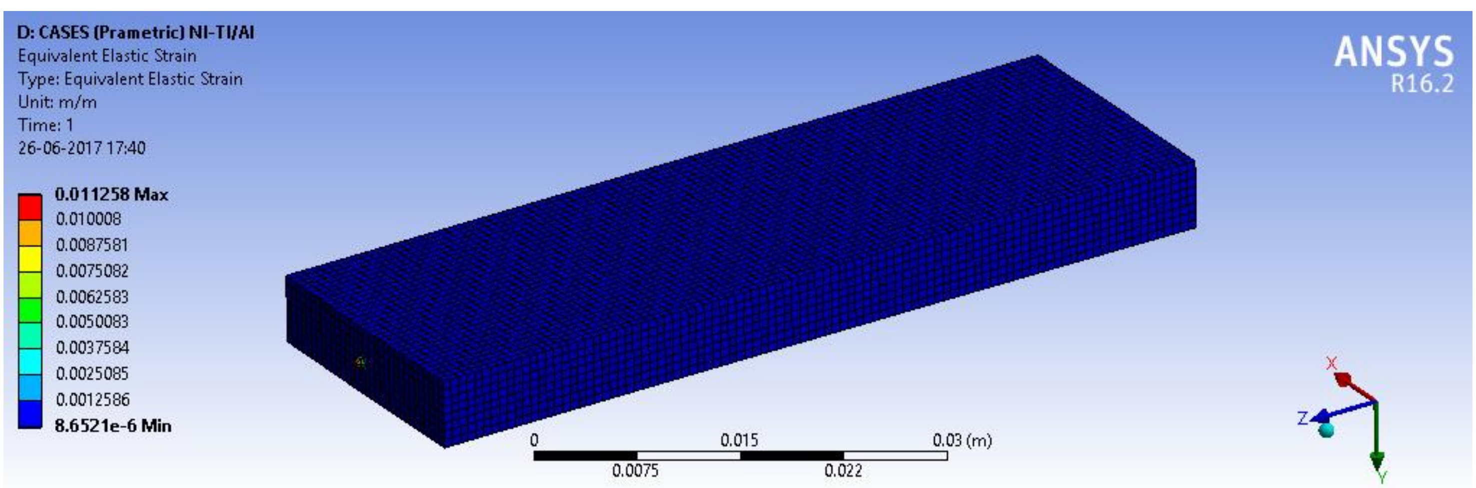

Fig 12. **Equivalent elastic strain**

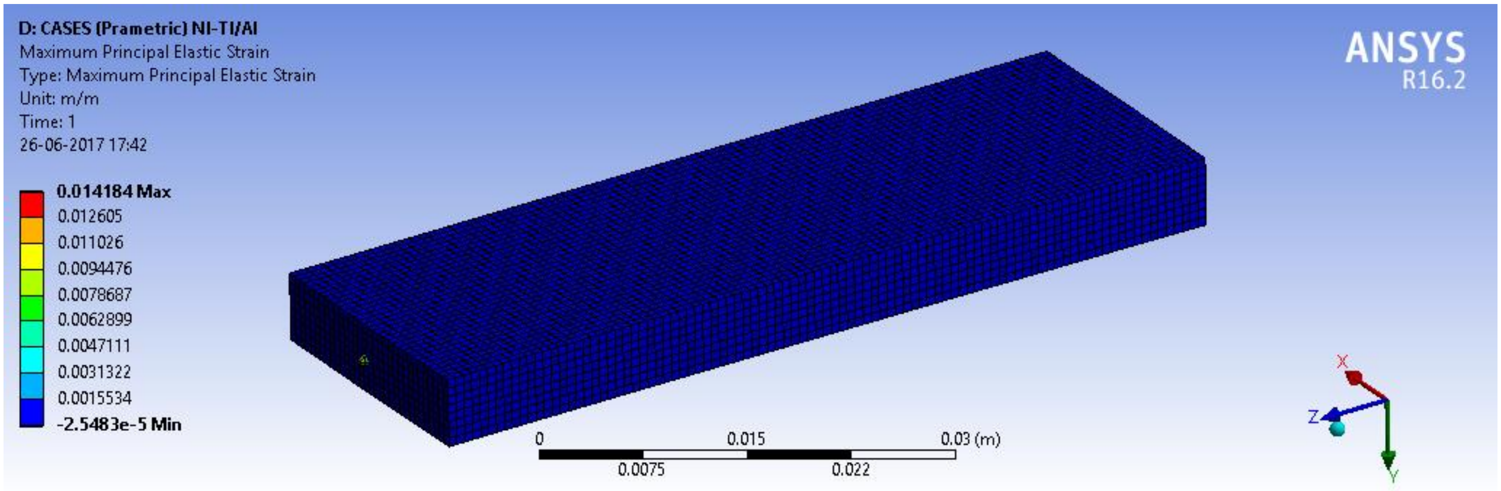

Fig 13. **Maximum principal elastic strain**

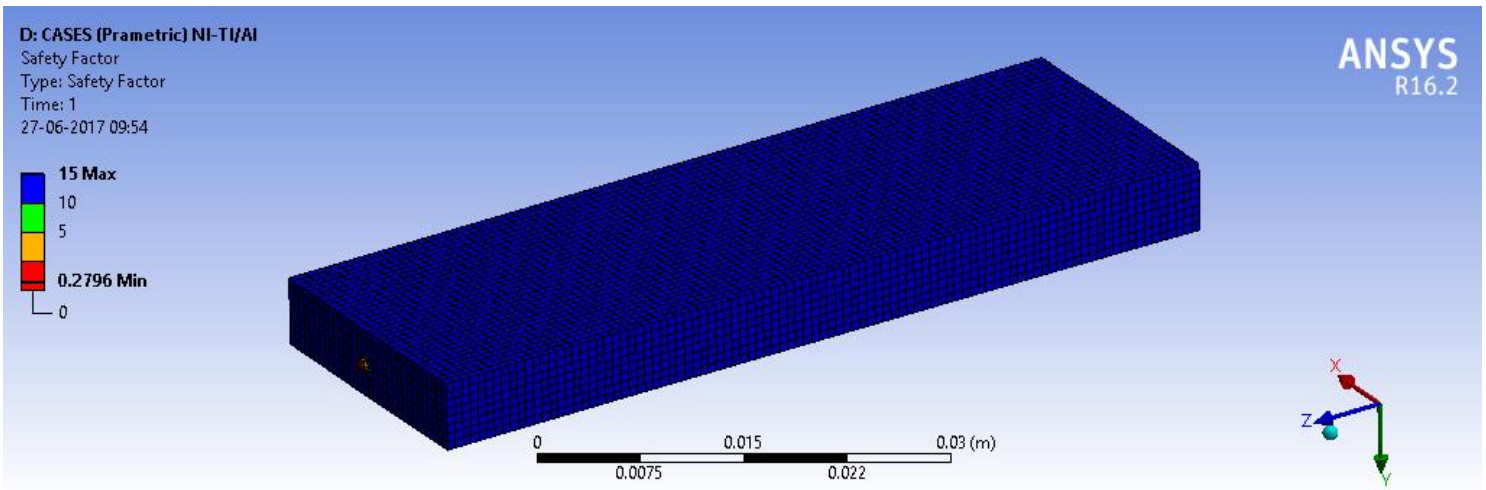

Fig 14. **Safety factor**

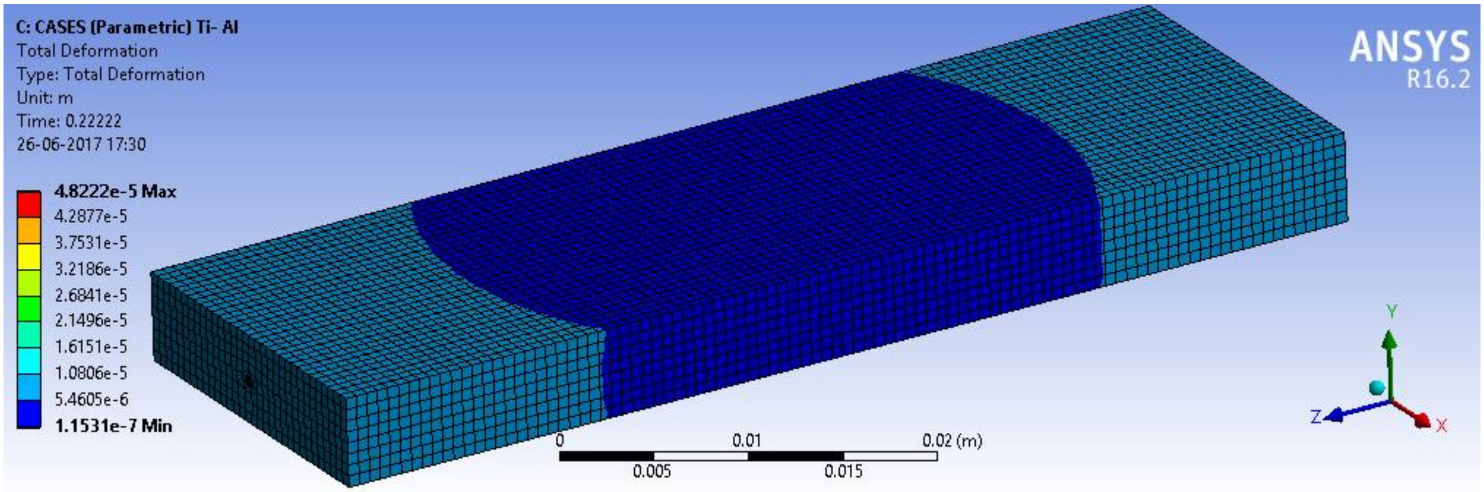

Fig.15 **Total deformation of Ti-Al**

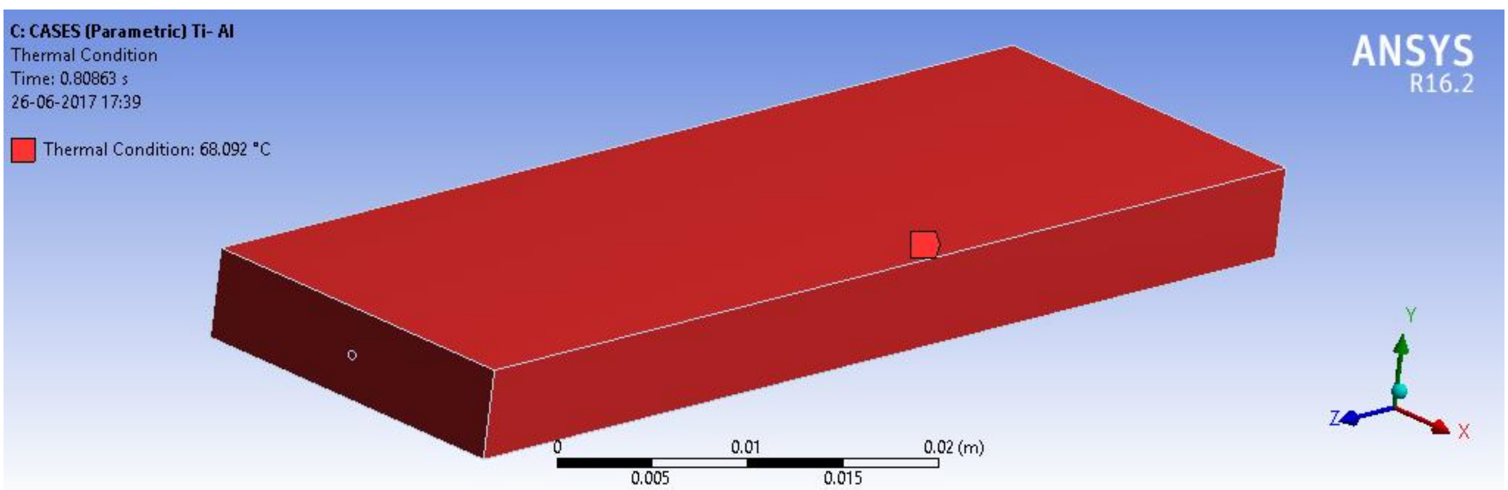

Fig.16 **Thermal condition of Ti-Al**

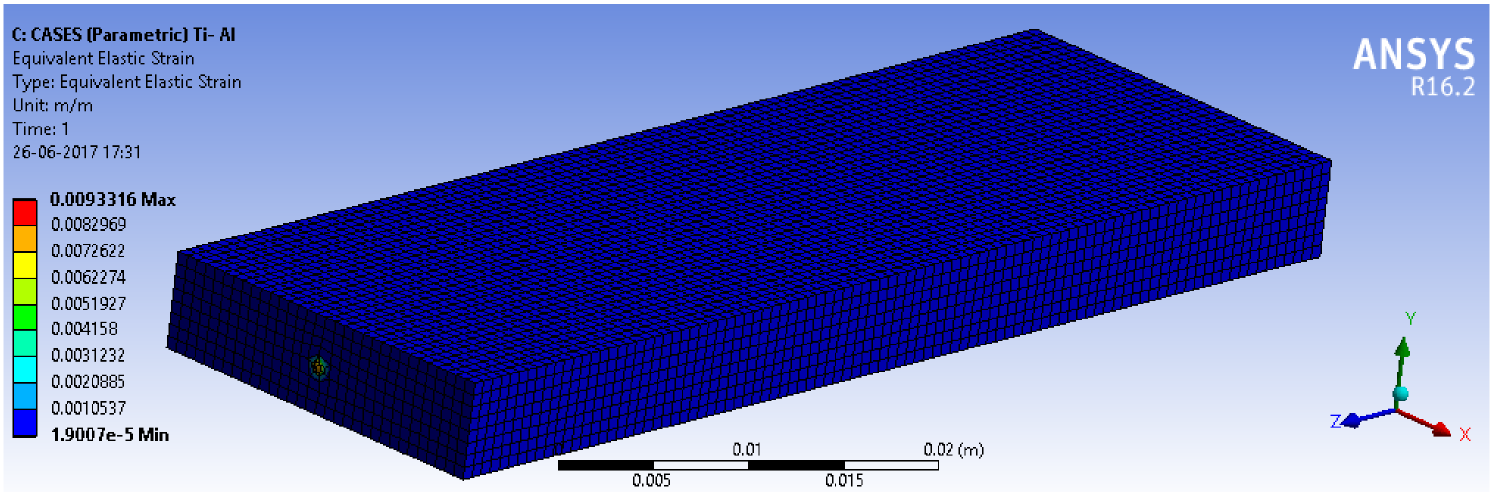

Fig.17 **Equivalent elastic strain of Ti-Al**

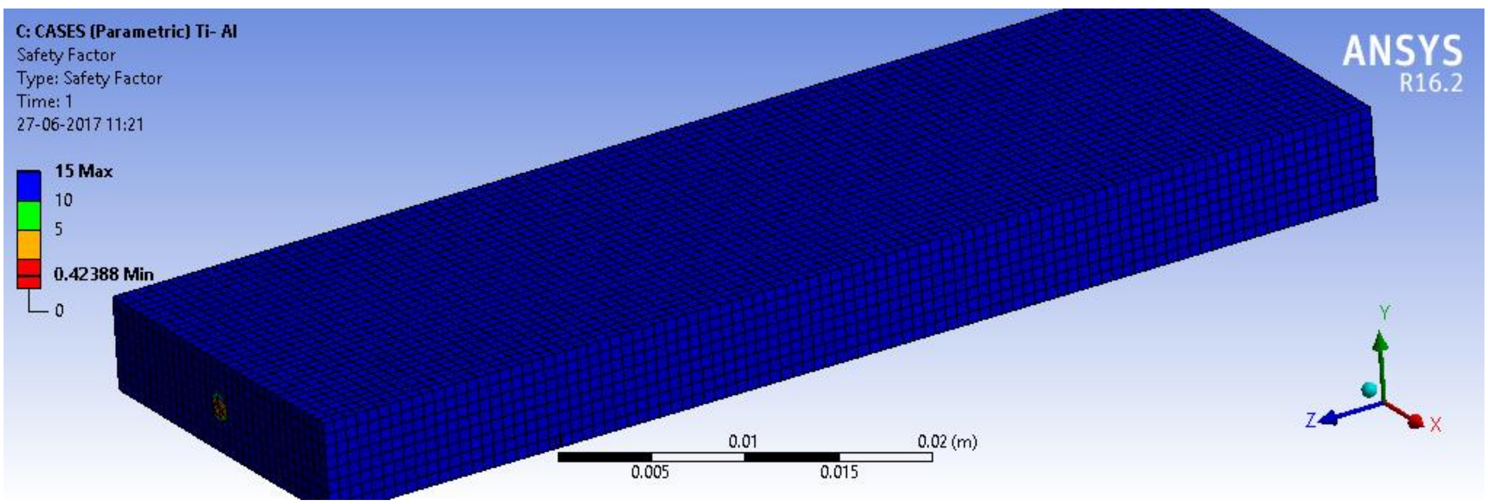

Fig.18 **Safety Factor of Ti-Al**

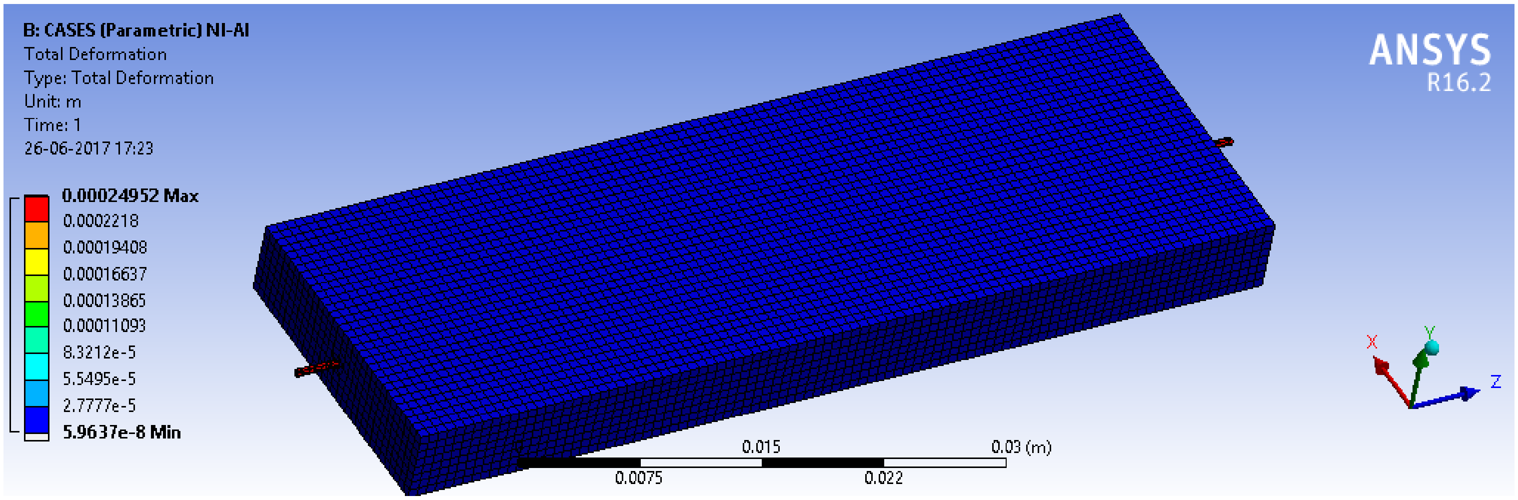

Fig.19 **Total deformation of Ni-Al**

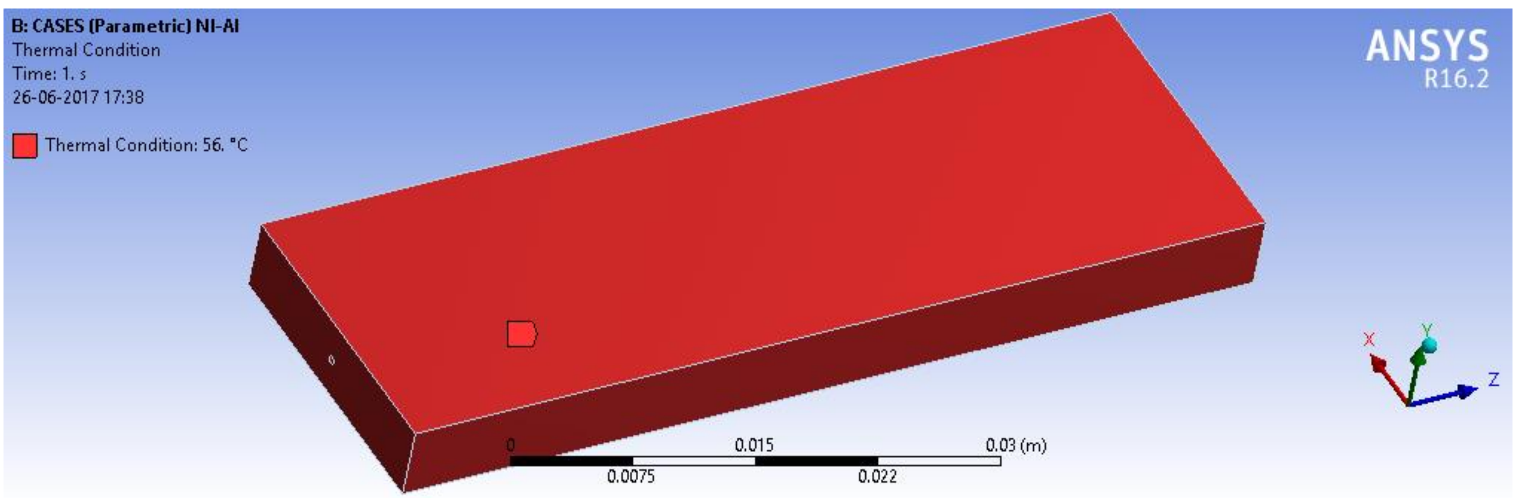

Fig.20 **Thermal condition of Ni-Al**

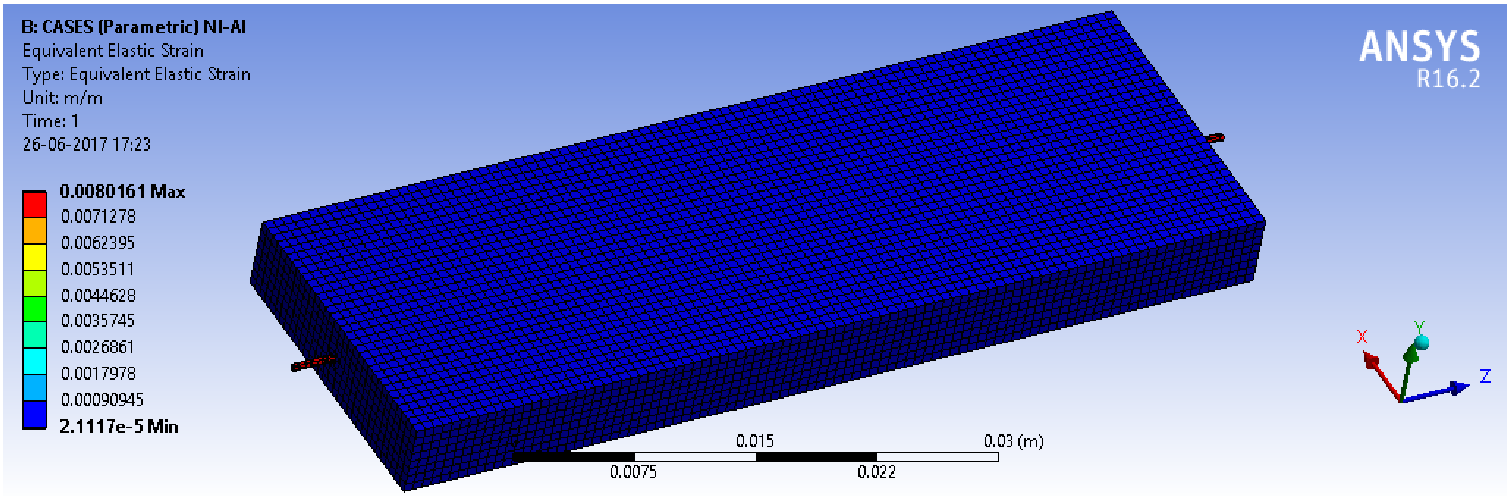

Fig.21 **Equivalent elastic strain of Ni-Al**

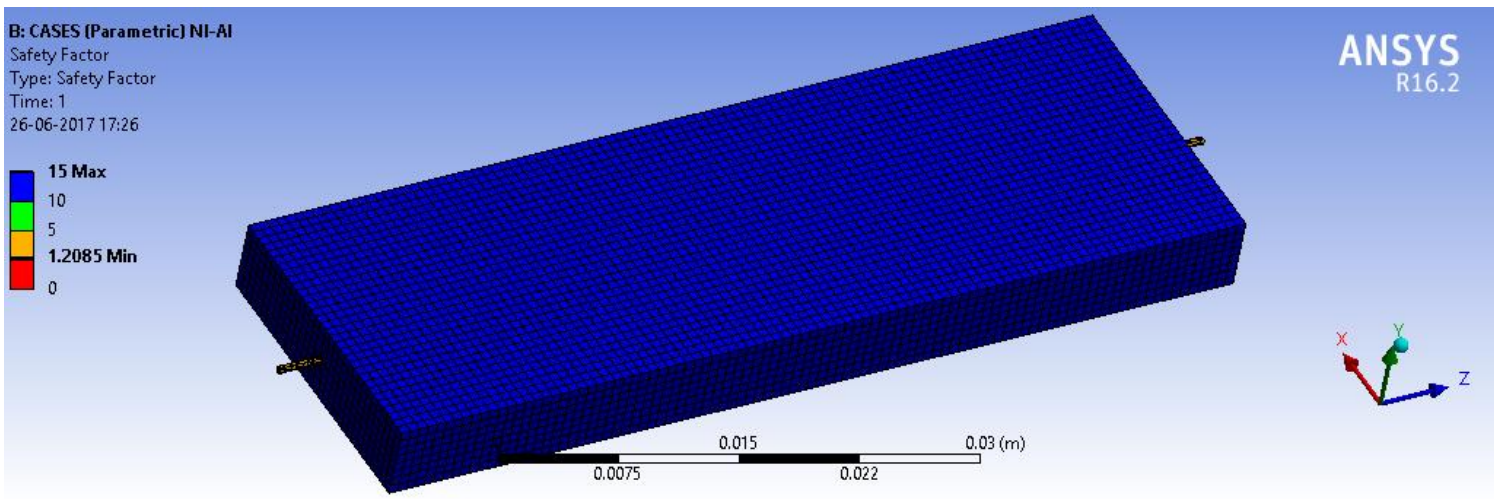

Fig.22 **Safety factor of Ni-Al**

4.2 Results and Discussion

Table 14. <u>Comparative study</u>

Composite	Object Name	Equivalent Elastic Strain	Total Deformation
Ni-Ti/Al	Minimum	$8.6521*10^{-6}$	$6.2432*10^{-8}$
	Maximum	0.011258	$2.454*10^{-5}$
Ti-Al	Minimum	$1.9007*10^{-5}$	$1.1531*10^{-7}$
	Maximum	0.0093316	$4.822*10^{-5}$
Ni-Al	Minimum	$2.1117*10^{-5}$	$5.9637*10^{-8}$
	Maximum	0.0080161	0.00024952

The three material composites were subjected to a loading cycle that ranges from 160 N to 256 N. The process induced reactions of NiTi/Al was stimulated simulated by ANSYS workbench version 16.2. Furthermore, two others composite, Ni/Al and Ti/Al, are also simulated and the eq. elastic strain that plays a role in reforming the alloy on removal of load is studied and their variation is plotted as below,

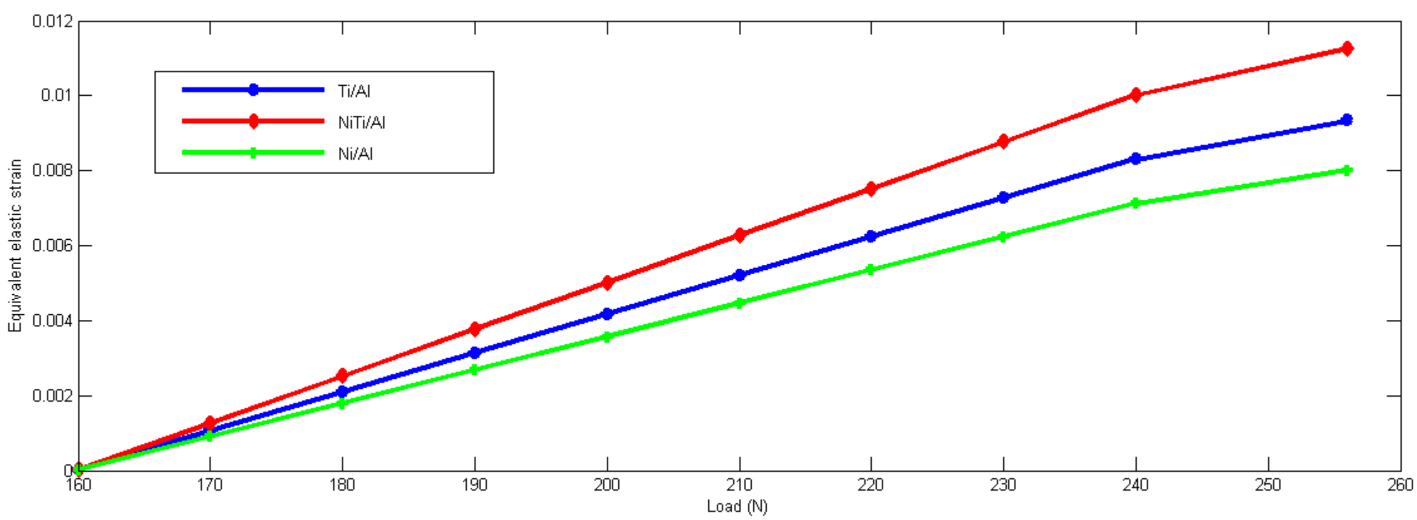

Fig 23. Equivalent elastic strain distribution with varying load in metal matrix composite

After simulation, the three types of composites are able to generate eq. elastic strain on Al matrix. The shape recovery on subjecting to thermal loading is quite enhanced in the NiTi/Al composite. The NiTi fibre shows increase of 13% higher eq elastic strain value than Ti/Al composite and 40% increase than Ni/Al composite. This is because of the mismatch of the SME and thermal expansion of the matrix (Al) and fibre (NiTi)

4.3 Conclusion.

The finite element analysis (FEA) of the metal matrix composite is carried out and the results are studied. The grid dependency test, considering a relevance factor of 100 during meshing are carried out during the design stage of the composite. This provides with enhanced shape memory effect in the fibre matrix composite.

Chapter 5

5.1 Conclusion & future scope.

The FEA of the Metal matrix composite is carried out and the results are studied. The grid dependency test was run and the relevance factor was considered to be 100 during simulation. Post simulation the three composites are able to generate eq. elastic strain on Al matrix. It sustains a load upto 256 N and requires less heating (351K) as compared to 363 K [17].

The study can be applied to other SMA’s and the scope of improvement in the SME on subjecting to thermal loading can be identified.

References

[1] Jani M., Leary J., Subic M., A. & Gibson M. A. (2014). A review of shape memory alloy research, applications and opportunities. Materials and Design

[2] Borden, Tom. "Shape-Memory Alloys: Forming a Tight Fit." Mechanical Engineering

[3] A.P. Markopoulos, I.S. Pressas, D.E. Manolakos, Manufacturing processes of shape memory alloys

[4] Hodgson, Darel E., W. H. Ming, and Robert J. Biermann. "Shape memory alloys." *ASM International, Metals Handbook, Tenth Edition.* 2 (1990): 897-902.

[5] Divringi, Kaan & Ozcan, Can, Advanced Shape Memory Alloy Material Models for ANSYS

[6] J.P. Oliveira, R.M. Miranda, F.M. Braz Fernandes, Welding and Joining of NiTi Shape Memory Alloys

[7] Shimamoto A., Ohkawara H., & Nogata F. (2004). Enhancement of mechanical strength by shape memory effect in TiNi fiber-reinforced composites. Engineering Fracture Mechanics 71 (4-6), 737-746.

[8] Watanabe Y., Miyazaki E., & Okada H. (2002). Enhanced mechanical properties of Fe-Mn-Si-Cr shape memory fiber/plaster smart composite. Materials Transactions 43(5), 974–983

[9] Jamian, Saifulnizan, Sato, Hisashi, Eri, Miura-Fujiwara, and Watanabe, Yoshimi Finite Element Analysis of Severe Plastic Deformation of Difficult-to-Work Material by Equal-Channel Angular Pressing at Ambient Temperature

[10] Choon, Tan Wee, Salleh, Abdul Saad, Jamian, Saifulnizan, and Mohd. Imran Ghazali Phase Transformation Temperatures for Shape Memory Alloy Wire

[11] Petrini, Lorenza Migliavacca, Francesco, Auricchio, Ferdinando Computational Studies of Shape Memory Alloy Behavior in Biomedical Applications.

[12] Xiaoyun, Song, Yan, Li, Fei, Zhang, Li, Shusuo NiTiAl Intermetallic Alloys Strengthened by Mo Replacement. Beijing University of Aeronautics and Astronautics.

[13] L.J. Zheng, F.X. Zhang, R.G. Ding, F.F. Wang, H. Zhang New phase and deformation behavior in directional solidified NiTiAl based intermetallic alloy upon cyclic tensile loading-unloading.

[14] V. I. Itin, V. E. Gyunter, S. A. Shabalovskaya, and R. L. C. Sachdeva Mechanical Properties and Shape Memory of Porous Nitinol.

[15] K.T. Liu, J.G. Duh, Hardness evolution of NiTi and NiTiAl thin films under various annealing temperatures

[16] K.T. Liu, J.G. Duh, Effect of aluminum on the corrosion behavior of NiTiAl thin films.

[17] Gashtia, S.O., Shokuhfara, A., Ebrahimi-Kahrizsangib, R., Nasiri-Tabrizi, B. Synthesis of nanocrystalline intermetallic compounds in Ni–Ti–Al system by mechanothermal method.

[18] Tang Tsz Loong, Saifulnizan Jamian, Al Emran Ismail, Nik Hisyammudin Muhd Nur, Yoshimi Watanabe Residual stresses in shape memory alloy fiber reinforced aluminium matrix composite

[19] Military Handbook: Metallic materials and elements for aerospace vehicle structures

[20] ASME boiler and pressure vessel code sec 8, div 2

[21] https://www.computationalfluiddynamics.com.au/convergence-and-mesh-independent-study/

Plagiarism Checker X Originality Report

Similarity Found: 18%

Date: Monday, July 03, 2017
Statistics: 958 words Plagiarized / 5048 Total words
Remarks: Medium Plagiarism Detected - Your Document needs Selective Improvement.
